Performance of Coded Multi-Carrier DS-CDMA System in Multi-Path Fading Channels

Qingxin Chen, Elvino S. Sousa, and Subbarayan Pasupathy
Department of Electrical and Computer Engineering
University of Toronto
Toronto, Canada, M5S 1A4
E-mail: sousa@comm.utoronto.ca

Abstract

Multi-carrier DS-CDMA has been considered as an effective scheme for reducing multiple access interference in the case of quasi-synchronous transmission. The scheme allows the reduction of multiple access interference by transferring the orthogonality property of the signals into the frequency domain where the orthogonality property is robust to relative chip offsets between the spreading codes of the various users. However in multi-path channels, the multi-carrier technique results in frequency non-selective fading in the sub-channels, due to the narrower bandwidth, hence a reduction of the capability of the spread spectrum signal to mitigate the effect of multi-path propagation. In this paper, we consider the use of a Reed-Muller code with soft decision decoding to regain the corresponding loss in performance, and compare the resulting system with a single carrier DS-CDMA system. The effect of system parameters such as the number of sub-channels is investigated through numerical calculation and simulation, from which a number of system design criteria are arrived at.

1 Introduction

The direct sequence code division multiple access (DS-CDMA) technique has been favourably considered for application in digital mobile cellular networks due to its potential to provide higher system capacity over conventional multiple access techniques, [1, 2]. Unlike FDMA and TDMA capacities which are mostly limited by the bandwidth, the capacity of a CDMA system is mainly restricted by its interference level. Any reduction in interference produces a direct and linear increase in system capacity [3].

Multiple access interference (MAI) caused by non-zero cross-correlation between different spreading sequences is the major type of interference limiting the CDMA system capacity. Much work has been done to characterize MAI, and to analyze and evaluate the CDMA system performance in the presence of MAI [4, 5]. Since the cross-correlation properties of most sets of spreading codes are either too complex to analyze or very difficult to compute when different transmissions are not synchronized, a random sequence model is usually assumed [4]. In the case of moderate to large processing gains, Gaussian distribution with variable variance is a good approximation for the MAI distribution [6].

One of the approaches to reduce MAI is to employ orthogonal spreading sequences, and try to synchronize the transmissions at the chip level (quasi-synchronization). However, this is generally difficult to achieve in multipoint-to-point systems, such as the reverse link (mobile-to-base) of a cellular system, due to a lack of synchronization of the various mobile terminals, and the variable transmission delays. In this paper, a multi-carrier DS-CDMA (MC-DS-CDMA) scheme is employed to facilitate the synchronization process, and thus reduce MAI.

Multi-carrier transmission technique has been introduced into DS-CDMA systems for reasons of high rate data transmission, bandwidth efficiency, frequency diversity, or interference reduction etc. So far we have seen at least two types of MC-DS-CDMA schemes. In the type I system, the serial data stream is first spread by a PN sequence, and then converted into N parallel chip sequences with each one modulating a different carrier. The number of carriers required is N, which equals the number of chips per data symbol. This type of system offers both the robustness of orthogonal modulation and the flexibility of the DS-CDMA scheme [7, 8, 9, 10, 11, 12, 13, 14]. In the type II MC-DS-CDMA system, which is of interest here, the serial data stream is first converted into M parallel data sub-streams, and each sub-stream is then spread by a PN sequence and transmitted over one of M sub-channels as narrow-band DS waveforms. The number of carriers required is M, which is usually much less than N [15]. While maintaining the overall data rate unchanged, this scheme lowers the chip rate in each sub-channel so that a longer chip time makes it easier to quasi-synchronize the transmissions. The multi-user interference can be effectively reduced in this type of system by applying orthogonal spreading sequences. In the rest of the paper, we refer to the type II system when MC-DS-CDMA system is mentioned.

The above gains in multi-user interference reduction occur, however, at the expense of a loss in frequency selectivity in the sub-channels, in the presence of multi-path fading, where the use of a wide-band signal along with a Rake receiver is a common approach. Although a frequency diversity technique which is equivalent to the use of a rate $\frac{1}{M}$ repetition code has been adopted in such a system[16, 17], it reduces the data rate by a factor of M. In this paper, we consider the use of a more sophisticated error control coding scheme with optimum soft decision decoding to regain the above loss in performance without reducing the data rate of the system. The performance of the coded MC-DS-CDMA scheme is compared with a single carrier DS-CDMA (SC-DS-CDMA) scheme utilizing a Rake receiver as suggested in [11].

The organization of the paper is as follows: in the next section, the models of system transmitter, channel, and receiver are described. In section 3 the decoded bit error probability is derived under certain assumptions, and a simulation scheme is constructed. Section 4 presents numerical and simulation results. In section 5 a few system design criteria are given as conclusions.

2 System Model

A model of the MC-DS-CDMA system for the k^{th} user of a CDMA system is shown in Fig. 1.

2.1 Transmitter Model

At the transmitter, the user's (coded and/or interleaved) data stream $d_k(t)$ is divided into M interleaved sub-streams and spread by a spreading sequence $c^k(t)$ to a fraction $1/M$ of the entire transmission bandwidth W. The resultant chip sequences are then

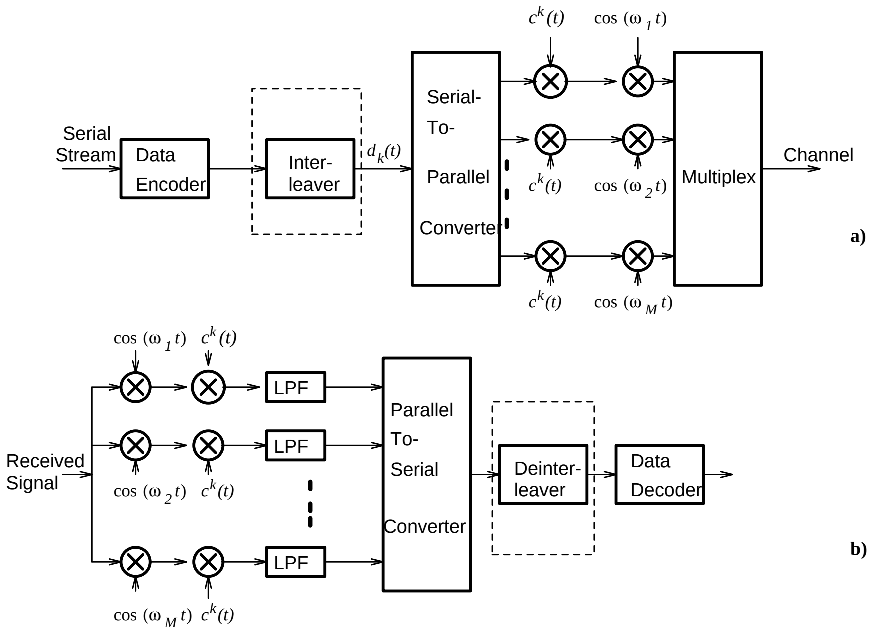

Figure 1: A multi-carrier direct-sequence spread spectrum system: a) Transmitter, b) Receiver.

used to modulate M carriers. The carrier frequencies $\omega_m, m = 1, 2, \cdots, M$ are equally spaced by the chip rate so that they are mutually orthogonal over one channel symbol interval T. Let R be the information rate and R_c be the error control code rate, then the channel symbol interval is

$$T = R_c/R. \tag{1}$$

Although a data encoder is often crucial for assuring acceptable performance in fading channels, the need for the interleaver depends on the channel characteristics and the multi-carrier scheme, which will be discussed later.

Assuming BPSK modulation, the transmitted signal is the sum of the signal streams from all the users across the sub-channels:

$$s(t) = \sum_{k=1}^{K} \sum_{m=1}^{M} \sqrt{2P_{k,m}} d_{k,m}(t - \epsilon_k) c^k(t - \epsilon_k) \cos(\omega_m t + \psi_k), \tag{2}$$

where $P_{k,m}$ is the transmitted power of the k^{th} user over the m^{th} sub-channel, $d_{k,m}(t)$ is the k^{th} user's m^{th} coded binary data sub-stream taking values ± 1 , and $c^k(t)$ is k^{th} user's spreading sequence whose chip time is

$$T_c = \frac{1}{W} \times M. \tag{3}$$

The quantities ϵ_k and ψ_k are the time and phase errors caused by imperfect synchronization. They are uniformly distributed in the intervals $[-\epsilon_D, \epsilon_D]$ and $[0, 2\pi]$, respectively. K is the total number of users.

2.2 Channel Model

The entire bandwidth available for multi-carrier transmission is usually much larger than the data rate. As suggested by [18], the channel for the k^{th} user is modeled as a linear filter with the complex-valued impulse response

$$p_k(t) = \sum_{l=0}^{L} \alpha_{k,l}\delta(t - \zeta_{k,l})\exp(j\phi_{k,l}), \tag{4}$$

where $\alpha_{k,l}$, $\zeta_{k,l}$ and $\phi_{k,l}$ are the path amplitude, time delay and signal phase in the l^{th} path, respectively. They are assumed constant over at least one symbol interval. The vectors $\vec{\alpha_k} = (\alpha_{k,1}, \alpha_{k,2}, \cdots, \alpha_{k,L})$, $\vec{\zeta_k} = (\zeta_{k,1}, \zeta_{k,2}, \cdots, \zeta_{k,L})$ and $\vec{\phi_k} = (\phi_{k,1}, \phi_{k,1}, \cdots, \phi_{k,L})$ are modeled as mutually independent random vectors with mutually independent components [19]. Let ζ_D be the range of $\zeta_{k,l}$, which is called the *delay spread*. The inverse of ζ_D is defined as the *channel coherence bandwidth* Δf_c. Multi-path signals are considered resolvable if the signal bandwidth is larger than Δf_c [20].

A practical DS spread spectrum system usually occupies a bandwidth much broader than Δf_c so that a Rake receiver can be used to combine multi-path signals and thus to optimize the performance [21]. However, in the MC-DS-CDMA system, data are transmitted over parallel sub-channels with bandwidth equal to a fraction of W. As indicated by the results in [15], to effectively reduce the MAI, the number of sub-channels should be chosen so that the time offset between received spreading sequences becomes a fraction of T_c, which in turn results in non-resolvable multi-path components. For the k^{th} user, the impulse response of the m^{th} sub-channel is given by

$$h_{k,m}(t) = \alpha_{k,m}\delta(t - \zeta_k)\exp(j\phi_{k,m}), \tag{5}$$

where $\alpha_{k,m}$ and $\phi_{k,m}$ are the combination of multiple paths in (4), and $\zeta_k \approx \zeta_{k,1} \approx \cdots \approx \zeta_{k,L}$ [18]. Variable ζ_k and vectors $\vec{\alpha_k} = (\alpha_{k,1}, \alpha_{k,2}, \cdots, \alpha_{k,M})$, and $\vec{\phi_k} = (\phi_{k,1}, \phi_{k,2}, \cdots, \phi_{k,M})$ are mutually independent. At the frequency of interest, we have $\mathcal{E}|\zeta_{k,i} - \zeta_{k,j}| \gg 1/\omega_m$, for $i \neq j$, so $\phi_{k,m}, m = 1, 2, \cdots, M$ can be treated as independent random variables. There may exist correlation between random variables $\alpha_{k,m}, m = 1, 2, \cdots, M$ depending on the sub-channel bandwidth relative to Δf_c.

In what follows, it can be seen that while model (5) is convenient for the purpose of analysis, model (4) is good for simulation, based on which narrow band models are derived and used for the comparison of different multi-carrier schemes.

Applying (5) to (2), the channel output is

$$r(t) = \sum_{k=1}^{K}\sum_{m=1}^{M} \sqrt{2P_{k,m}}\alpha_{k,m}d_{k,m}(t - \tau_k)c^k(t - \tau_k)\cos(\omega_m t + \theta_{k,m}) + n(t). \tag{6}$$

where $n(t)$ is a AWGN process with power spectral density $N_0/2$. The faded signal amplitude is denoted by $\gamma_{k,m}$, i.e. $\gamma_{k,m} = \sqrt{2P_{k,m}}\alpha_{k,m}$. The time offset τ_k between signal sub-streams results from both synchronization error and multi-path delay, i.e. $\tau_k = \epsilon_k + \zeta_k$. Similarly, $\theta_{k,m} = \psi_k + \phi_{k,m}$.

2.3 Receiver Model

There are M branches in the receiver with each detecting the data sub-stream from one sub-channel. We are concerned with the first user's m_0^{th} data sub-stream. Assuming that the time variation of fading is slow enough so that the arrival time and phase of the desired signal can be acquired (the tracking system is not included in the system diagram, Fig. 1), we may set τ_1 and θ_{1,m_0} to zero. The output of the m_0^{th} low pass filter (LPF) at the sampling point is therefore

$$y_{1,m_0}(T) = \pm\frac{\gamma_{1,m_0}T}{2} + I_{m_0} + J_{m_0} + \eta, \tag{7}$$

where I_{m_0} and J_{m_0} are the MAI components from inside and outside the m_0^{th} sub-channel, respectively, and η is the noise term. The sign $\pm$ depends on the data bit value.

Considering a $[0,T]$ integrator as the LPF, I_{m_0} and J_{m_0} can be written as

$$I_{m_0} = \sum_{k=2}^{K}\int_0^T \frac{\gamma_{k,m_0}}{2}\cos(\theta_{k,m_0})d_{k,m_0}(t-\tau_k)c^k(t-\tau_k)c^1(t)dt, \tag{8}$$

and

$$J_{m_0} = \sum_{k=2}^{K}\sum_{m=1,m\neq m_0}^{M}\int_0^T \frac{\gamma_{k,m}}{2}\cos(\omega_d t + \theta_{k,m}) \times d_{k,m}(t-\tau_k)c^k(t-\tau_k)c^1(t)dt, \tag{9}$$

where $\omega_d = \omega_{m_0} - \omega_m$, and η is

$$\eta = \int_0^T n(t)\cos(\omega_{m_0}t)c_1(t)dt, \tag{10}$$

which is a zero mean Gaussian random variable with variance $\sigma_\eta^2 = \frac{N_0 T}{4}$.

Soft decision decoding is performed on the serially converted (and interleaved, if necessary) data stream to compensate for the performance degradation due to channel fading.

3 BER Performance

In this section, we investigate the MC-DS-CDMA system's performance measured by the bit error rate (BER) through analysis and simulation.

3.1 Analysis

The BER is derived under the following assumptions : 1) Orthogonal spreading sequences with rectangular pulse shape are applied. 2) $\tau_k, k = 1, \cdots, K$ are independent random variables uniformly distributed in $[-\tau_D, \tau_D]$, where $\tau_D = \epsilon_D + \zeta_D$. Given W and τ_D, M is chosen so that $\tau_D \leq T_c$. 3) It is assumed that the fading parameters of the desired user can be perfectly estimated so that the coherent detection and optimum soft decision decoding could be carried out at the receiver. Furthermore, to make the problem analytically tractable, we model the fading amplitudes as independent Rayleigh random variables with equal second moments [12]. This model is a good approximation of the practical situations where $\Delta f_c \approx W/M$ or ideal interleaving is applied. The effect of correlated fading amplitudes over sub-channels is investigated later through simulation. 4) $\theta_{k,m}, k = 1, \cdots, K, m = 1, \cdots, M$ are independent random variables uniformly distributed in $[0, 2\pi]$.

Let $c^k(t) = \sum_{n=-\infty}^{\infty} c_n^k \rho(t - nT_c)$, where $\rho(t)$ is 1, for $t \in [0, T_c]$ and 0 otherwise. Writing $\hat{c}^k(t) = c^k(t) d_{k,m_0}(t)$, we obtain the following from (8)

$$\begin{aligned} I_{m_0} &= \sum_{k=2}^{K} \sum_i \sum_j \hat{c}_i^k c_j^1 \int_0^T \frac{\gamma_{k,m_0}}{2} \cos(\theta_{k,m_0}) \rho(t - iT_c - \tau_k) \rho(t - jT_c) dt \\ &= \sum_{k=2}^{K} \frac{\gamma_{k,m_0}}{2} \cos(\theta_{k,m_0}) \sum_i \sum_{j=0}^{N-1} \hat{c}_i^k c_j^1 \int_{-\infty}^{\infty} \rho[t + (j-i)T_c - \tau_k] \rho(t) dt \end{aligned} \tag{11}$$

where N is the spread spectrum processing gain defined as $N = \lfloor T/T_c \rfloor$. Since $\sum_i \sum_j \hat{c}_i^k c_j^1 = 0$ when $i = j$, for orthogonal spreading sequences, the above integration is non-zero only when $j = i + 1$. We have

$$I_{m_0} = \sum_{k=2}^{K} \frac{\gamma_{k,m_0}}{2} \cos(\theta_{k,m_0}) \tau_k \sum_{j=0}^{N-1} \hat{c}_{j-1}^k c_j^1, \tag{12}$$

$c_{-n}^k = c_{N-n}^k$, for $0 \leq n \leq N-1$.

As mentioned in section 1, it is difficult to analyze the cross-correlation properties of most practically used spreading sequences [22]. In the case of sequences with long period the sequences may be modelled as Bernoulli processes for the purpose of analysis. The correlation term $\sum_{j=0}^{N-1} \hat{c}_{j-1}^k c_j^1$ is a sum of ± 1 terms. When N is moderate to large, we may invoke the central limit theorem and model each term in the sum of (12) as having a Gaussian distribution conditioned on θ_{k,m_0}, γ_{k,m_0} and τ_k. The distribution has zero mean and the variance of I_{m_0} is

$$V(I_{m_0}) = \sum_{k=2}^{K} \frac{\gamma_{k,m_0}^2}{4} N \tau_k^2 \cos^2(\theta_{k,m_0}), \tag{13}$$

which is a variable. Averaging (13) over the probability density function (p.d.f.) of θ_{k,m_0}, γ_{k,m_0} and τ_k, the expected value of $V(I_{m_0})$ is

$$\bar{V}(I_{m_0}) = \mathcal{E}(V(I_{m_0})) = \frac{(K-1)PNT_c^2 D_m^2}{12}, \tag{14}$$

where $P = \mathcal{E}(\gamma_{k,m_0}^2)/2$, which is the received signal power. P is constant for every signal stream when perfect power control is assumed. $D_m = \tau_D/T_c$ is the normalized range of time offset. It is seen that I_{m_0} does not depend on m_0, therefore the subscript m_0 will be omitted in the sequel, and the average variance of I will be simply denoted as V_I.

Similarly, (9) can be simplified as follows

$$
\begin{aligned}
J_{m_0} &= \sum_{k=2}^{K} \sum_{\substack{m=1 \\ m \neq m_0}}^{M} \frac{\gamma_{k,m}}{2} \sum_i \sum_{j=0}^{N-1} \hat{c}_i^k c_j^1 \int_{-\infty}^{\infty} \cos(\omega_d t + \theta_{k,m}) \rho[t + (j-i)T_c - \tau_k] \rho(t) dt \\
&= \sum_{k=2}^{K} \sum_{\substack{m=1 \\ m \neq m_0}}^{M} \frac{\gamma_{k,m}}{2} \int_0^{\tau_k} \cos(\omega_d t + \theta_{k,m}) dt \sum_{j=0}^{N-1} \hat{c}_{j-1}^k c_j^1 \\
&= \sum_{k=2}^{K} \sum_{\substack{m=1 \\ m \neq m_0}}^{M} \frac{\gamma_{k,m} [\sin(\omega_d \tau_k + \theta_{k,m}) - \sin\theta_{k,m}]}{2\omega_d} \sum_{j=0}^{N-1} \hat{c}_{j-1}^k c_j^1 .
\end{aligned} \tag{15}
$$

Following the same arguments for deriving $V(I_{m_0})$, we can approximate J_{m_0} as having a compound Gaussian distribution with variable variance given by

$$
V(J_{m_0}) = \sum_{k=2}^{K} \sum_{\substack{m=1 \\ m \neq m_0}}^{M} \frac{\gamma_{k,m_0}^2}{4} N \left[\frac{\sin(\omega_d \tau_k + \theta_{k,m}) - \sin\theta_{k,m}}{\omega_d} \right]^2 , \tag{16}
$$

and the average of $V(J_{m_0})$ is given by

$$
\begin{aligned}
\bar{V}(J_{m_0}) &= \mathcal{E}(V(J_{m_0})) \\
&= \sum_{\substack{m=1 \\ m \neq m_0}}^{M} \frac{(K-1)NPT_c^2}{8\pi^2 (m-m_0)^2} \mathrm{sinc}[2(m-m_0)D_m].
\end{aligned} \tag{17}
$$

Let $y_{1,m_j}, j = 1, \cdots, n_c$, represent the n_c LPF outputs for one particular code word. n_c is the length of the code. The optimum decoder combines the LPF outputs and forms the N_c decision variables

$$
U_i = \sum_{j=1}^{n_c} (2c_{ij} - 1) \gamma_{1,m_{ij}} y_{1,m_{ij}}, \qquad i = 1, 2, \cdots, N_c, \tag{18}
$$

where c_{ij} denotes the bit in the j^{th} position of the i^{th} code word, m_{ij} denotes the sub-channel number for transmitting c_{ij}, and N_c, the total number of code words.

Assuming the code word C_1 is transmitted, for correct decoding, U_1 must exceed all other decision variables $U_i, i = 2, 3, \cdots, N_c$. Let $s_i = \{j : c_{1j} \neq c_{ij}\}$,

$$
\mu_i = U_1 - U_i = \sum_{j \in s_i} [\gamma_{1,m_{1j}}^2 T + 2\gamma_{1,m_{1j}} (I + J_{m_{1j}} + \eta)]. \tag{19}
$$

Instead of attempting to derive the exact error probability, we resort to a union bound. Let $p_i = \mathrm{P}(\mu_i < 0)$, which is the probability of C_1 being decoded as C_i. The code symbol error probability can be bounded as

$$p_s \leq \sum_{i=2}^{N_c} p_i. \tag{20}$$

It is observed that p_i depends not only on the Hamming distance between C_1 and C_i, but also on the position of sub-channels over which these different bits are transmitted because $V(J_{m_0})$ is a function of m_0. However, from the system performance point of view, we interested in the average error probability. To find the average decoded error probability, we replace the term $V(J_{m_0})$ by its average which is

$$V_J = \frac{1}{M} \sum_{m_0=1}^{M} V(J_{m_0}), \tag{21}$$

and the minimum Hamming distance d_{min} is assumed between every pair of code words. For orthogonal codes like the Reed-Muller (RM) code used in this scheme, the equal distance assumption turns out to be exact.

Under the above assumptions and conditioned on $\gamma_{1,m_{1j}}, j = 1, \cdots, d_{min}$, μ_i is a Gaussian random variable with mean

$$\mathcal{E}(\mu_i) = T \sum_{j=1}^{d_{min}} \gamma_{1,m_{1j}}^2, \tag{22}$$

and variance

$$V(\mu_i) = 4[V_I + V_J + \sigma_\eta^2] \sum_{j=1}^{d_{min}} \gamma_{1,m_{1j}}^2. \tag{23}$$

Letting $\Gamma_{1,1} = \sum_{j=1}^{d_{min}} \gamma_{1,m_{1j}}^2$, the conditional error probability is given by

$$p_i(\lambda_s) = \frac{1}{2} erfc\sqrt{\lambda_s}, \tag{24}$$

where λ_s is defined as

$$\lambda_s = \frac{T^2 \Gamma_{1,1}}{8[V_I + V_J + \sigma_\eta^2]}. \tag{25}$$

Since we are only concerned with the average system BER over a long period of transmission, the average interference variances V_I and V_J are used in expressing λ_s, which approximates the average effect of the interferences on the system performance. To find the unconditional error probability p_i, we need to find the p.d.f. of λ_s. This is generally difficult even under the Rayleigh assumption because fading amplitudes may be correlated. Here we have assumed that $\gamma_{1,m_{1j}}, j = 1, \cdots, d_{min}$ are independent Rayleigh random variables, and under the above assumption, λ_s is a chi-square-distributed random variable with $2d_{min}$ degrees of freedom. Its p.d.f. is written as

$$f(\lambda_s) = \frac{1}{(d_{min}-1)!\lambda_b^{d_{min}}} \lambda_s^{d_{min}-1} \exp(-\lambda_s/\lambda_b), \tag{26}$$

where λ_b is defined as

$$\lambda_b = \frac{PT^2}{8[V_I + V_J + \sigma_\eta^2]}. \tag{27}$$

This is the average signal-to-noise-plus-interference-ratio (SINR) per sub-channel, which can be further expressed as

$$\lambda_b = \frac{1}{\frac{1}{\mathrm{SIR}} + \frac{2}{\mathrm{SNR}}}, \tag{28}$$

where SIR is defined as the average signal-to-interference-ratio per sub-channel

$$\begin{aligned} \mathrm{SIR} &= \frac{PT}{[8(V_I + V_J)/T]}, \\ &= \frac{R_c E_b}{[8(V_I + V_J)/T]}, \end{aligned} \tag{29}$$

Here E_b is energy per information bit, and R_c is the code rate. SNR is the average signal-to-noise-ratio per sub-channel

$$\mathrm{SNR} = \frac{PT}{N_0} = \frac{R_c E_b}{N_0}. \tag{30}$$

Averaging (24) over (26) yields the following

$$p_i = \int_0^\infty p_i(\lambda_s) f(\lambda_s) d\lambda_s. \tag{31}$$

The closed-form solution for (31) can be expressed as [20]

$$p_i = \left(\frac{1-\nu}{2}\right)^{d_{min}} \sum_{l=0}^{d_{min}-1} \begin{pmatrix} d_{min} - 1 + l \\ l \end{pmatrix} \left(\frac{1+\nu}{2}\right)^l, \tag{32}$$

where, by definition

$$\nu = \sqrt{\frac{\lambda_b}{1+\lambda_b}}. \tag{33}$$

The decoded bit error probability is approximately[20]

$$P_e \approx \frac{1}{2} p_s = \frac{N_c - 1}{2} p_i. \tag{34}$$

The BER derived above will be used to evaluate the system performance in the next section.

3.2 Simulation

In section 3.1, the BER was derived under the assumption that fading amplitudes are uncorrelated. In fact, to effectively reduce the MAI, the sub-channel chip time T_c is usually chosen to be larger than the maximum time offset τ_D, i.e. larger than the delay spread ζ_D. There exists a correlation between fading amplitudes and this correlation becomes stronger when the sub-channel bandwidth decreases. The purpose of the simulation is to find out how correlated fading affects the system performance, and to gain additional insights into the system behaviour.

The mathematical model for our simulation is given by (4). The parameter L is set to 3 without much loss of generality. For the k^{th} user, the channel is characterized by a set of fading amplitudes $\{\alpha_k\}_1^3$, path delays $\{\tau_k\}_1^3$, path phases $\{\phi_k\}_1^3$ and the additive noise $n(t)$. The parameters in each set are assumed to be mutually independent with independent components. The $\{\alpha_k\}_1^3$ have a Rayleigh distribution with unit second moment, $\{\tau_k\}_1^3$ are uniformly distributed in $[-\tau_D, \tau_D]$, where τ_D is a simulation parameter, and $\{\phi_k\}_1^3$ are uniformly distributed in $[0, 2\pi]$. The noise strength depends on the specified SNR.

The simulated channel is centered at 910 MHz with a bandwidth of 1.25 MHz. The data rate is 8 Kbps, which is equal to the output of a full rate vocoder. This allows for a maximum spread spectrum processing gain of about 156. With an error control code of rate R_c, the number of chips per channel symbol is reduced to $156 \times R_c$, i.e., 78 for a half rate RM code. To create the average effect, the spreading sequences from a set of N orthogonal sequences are randomly assigned to the users during each transmission. The number of active users in the system and the number of sub-channels are simulation parameters.

The method to derive the sub-channel parameters from the broadband channel model is described as follows: We first generate the set of random parameters $\{\alpha_k\}_1^3$, $\{\tau_k\}_1^3$, and $\{\phi_k\}_1^3$. Then the Fourier transform of (4) is found to be $H_k(j\omega)$, and $H(j\omega)$ is chopped into M bands representing the frequency response of each sub-channel

$$H_{k,m}(j\omega) = \begin{cases} H(j\omega) & \text{if } \omega \in B_m \\ 0 & \text{otherwise,} \end{cases} \tag{35}$$

where B_m is the frequency interval of the m^{th} sub-channel.

In principle, the time domain description of the sub-channel can be obtained as the inverse Fourier transform of $H_{k,m}(j\omega)$, which does not necessarily comply with (5). However, for the purpose of simulation, the model given by (5) is considered sufficient, and with which, we wish to approximate the time domain impulse response of $H_{k,m}(j\omega)$.

Rewrite $H_{k,m}(j\omega)$ as $|H_{k,m}(j\omega)|\exp[j\phi_{k,m}(\omega)]$, then the parameters in (5) are extracted as follows

$$\alpha_{k,m} = \mathcal{E}(|H_{k,m}(j\omega)|), \tag{36}$$
$$\phi_{k,m} = \mathcal{E}(\phi_{k,m}(\omega)), \tag{37}$$

where the expectation is over the entire sub-channel frequency band. The path delay τ_k is approximately the average of all path delays.

In the simulation, new channel parameters are generated during each transmission, i.e., serially transmitted code symbols go through independent fading channels. By doing this, we are assuming that the coherence time of the channel is equal to one symbol interval so that we could consider transmitting the code symbol serially as the interleaving method. In practice, the coherence time might be longer for slower fading channels and a more sophisticated interleaving technique could be applied.

In the simulation, the all-zero code word is transmitted repeatedly, and the received code words with Hamming weight exceeding the error control capability are considered erroneous. Simulations are run under different choices of τ_D and M to investigate the effect of these parameters on the system performance. For each set of parameters, 10^4 code words are transmitted and decoded. The code word error probability is calculated as the ratio of the number of erroneous code words to the number of code words transmitted. The bit error probability is easily obtained as approximately half of the code word error probability (34).

4 Numerical and Simulation Results

The first order RM code of parameter $(2^n, n+1)$ is chosen for numerical evaluation and simulation. This choice of code is based on practical considerations since the 1st order RM code can be decoded using a Fast Hadamard Transform algorithm. An RM code of length 2^n with minimum distance 2^{n-1} offers better error control capability than the frequently used BCH code [23]. The drawback that might have prevented it from wider application is its relatively low code rate which results in large signal bandwidth expansion. However, this is not an issue in the DS system where the transmission bandwidth available is normally much larger than the actual signal bandwidth.

In Fig. 2 and Fig. 3, the BER performance of the MC-DS-CDMA system is compared with a SC-DS-CDMA system employing a Rake receiver, which almost fully compensates the performance loss due to multi-path fading. Fig. 2 shows that, although the MC-DS-CDMA system does not outperform the SC-DS-CDMA system when coding is not applied, its performance is much less sensitive to the increase of user number. This is because a MC-DS-CDMA system suppresses the MAI effectively. The major source of performance loss comes from the flat fading over each sub-channel which can not be equalized as it is in the SC-DS-CDMA system. However, error control coding can be very effective for combating the fading. Fig. 3 shows that the $(8,4)$ RM code brings down the error probability of a MC-DS-CDMA system by a considerably larger margin than it does with the SC-DS-CDMA system. It is seen that the MC-DS-CDMA system can actually outperform the SC-DS-CDMA system at a high user capacity.

A rectangular chip pulse was assumed throughout the analysis, however any other square root Nyquist I pulse may be used. In practice, a band-limited chip pulse is preferable for mitigating the inter-sub-channel interference. Fig. 4 shows the performance improvement by using a minimum bandwidth **sinc** pulse which eliminates the inter-sub-channel interference completely.

The above results are obtained with the assumption that fading amplitudes over sub-channels are independent. Fig. 5 presents the performance in the other extreme case where path amplitudes are totally correlated. It is seen that the correlation could deteriorate the performance considerably and therefore an interleaving technique should be applied. The performance of a practical system is expected to fall between these two extremes.

We also investigate the effect of the number of sub-channels M on the system perfor-

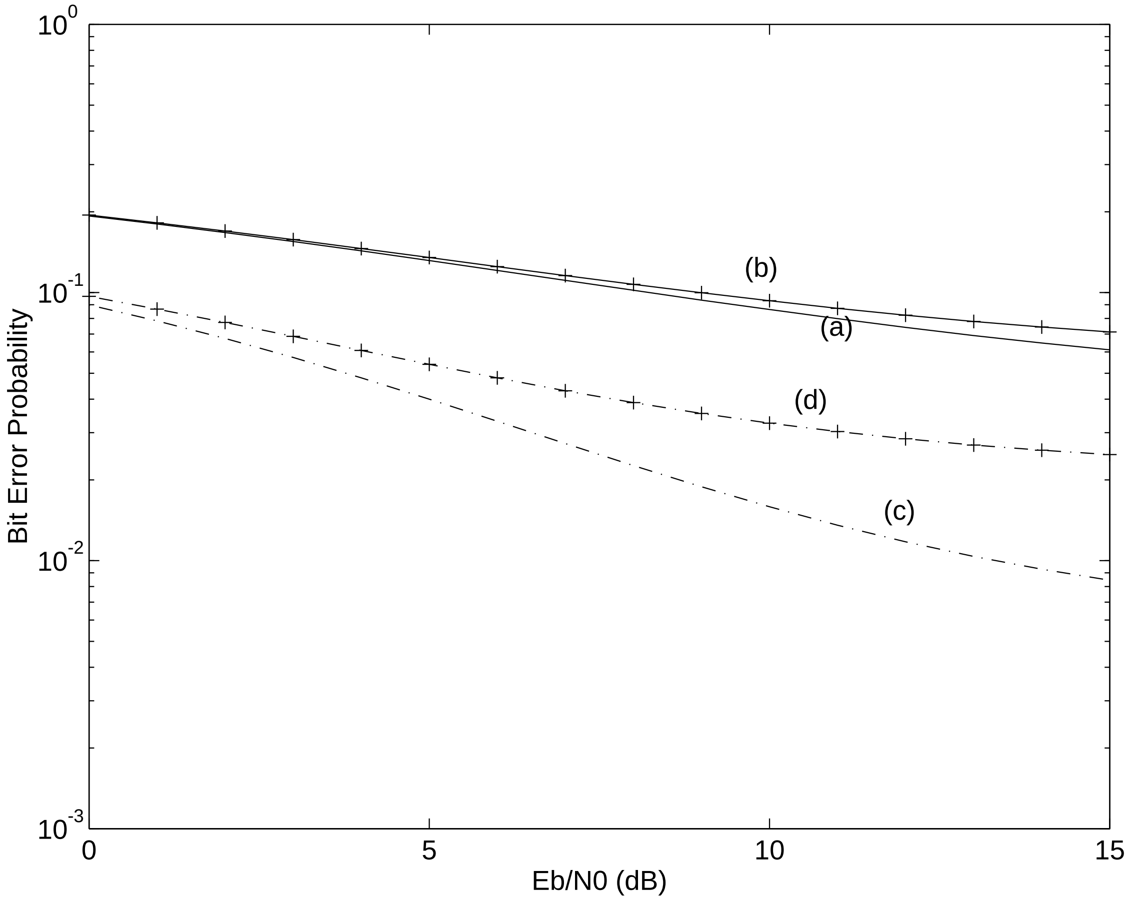

Figure 2: Comparison of performance sensitivities to the variation of the number of users between MC-DS-CDMA and SC-DS-CDMA systems. $M = 8$, $\tau_D = 4/W$. a),b) MC-DS-CDMA system with 40 and 70 users, respectively. c),d) SC-DS-CDMA system with 40 and 70 users, respectively.

mance. It is indicated in [15] that increasing the number of sub-channels can always lead to performance gain in AWGN channels. The results in Fig. 6 seem to have extended this conclusion to the multi-path fading channels. Nevertheless, we realize that this result is subject to the assumption we made on the independence of fading amplitudes. We expect to gain a better understanding of the effect of parameter M on the system performance through the process of simulation.

The simulation results are displayed in Figs. 7, 8, and 9. In Fig. 7, the delay spread is almost equal to the chip time, i.e., the coherence bandwidth is approximately equal to the sub-channel bandwidth so that the correlation between sub-channels is weak. It is noticed that while the interleaving technique makes little improvement over the performance in this case, an increased number of sub-channels steadily brings down the error probability. In Fig. 8, another extreme is tested where the coherence bandwidth is nearly equal to the entire channel bandwidth. It is shown that the interleaving technique improves the performance significantly. A phenomenon which did not appear in Fig. 7 is that when

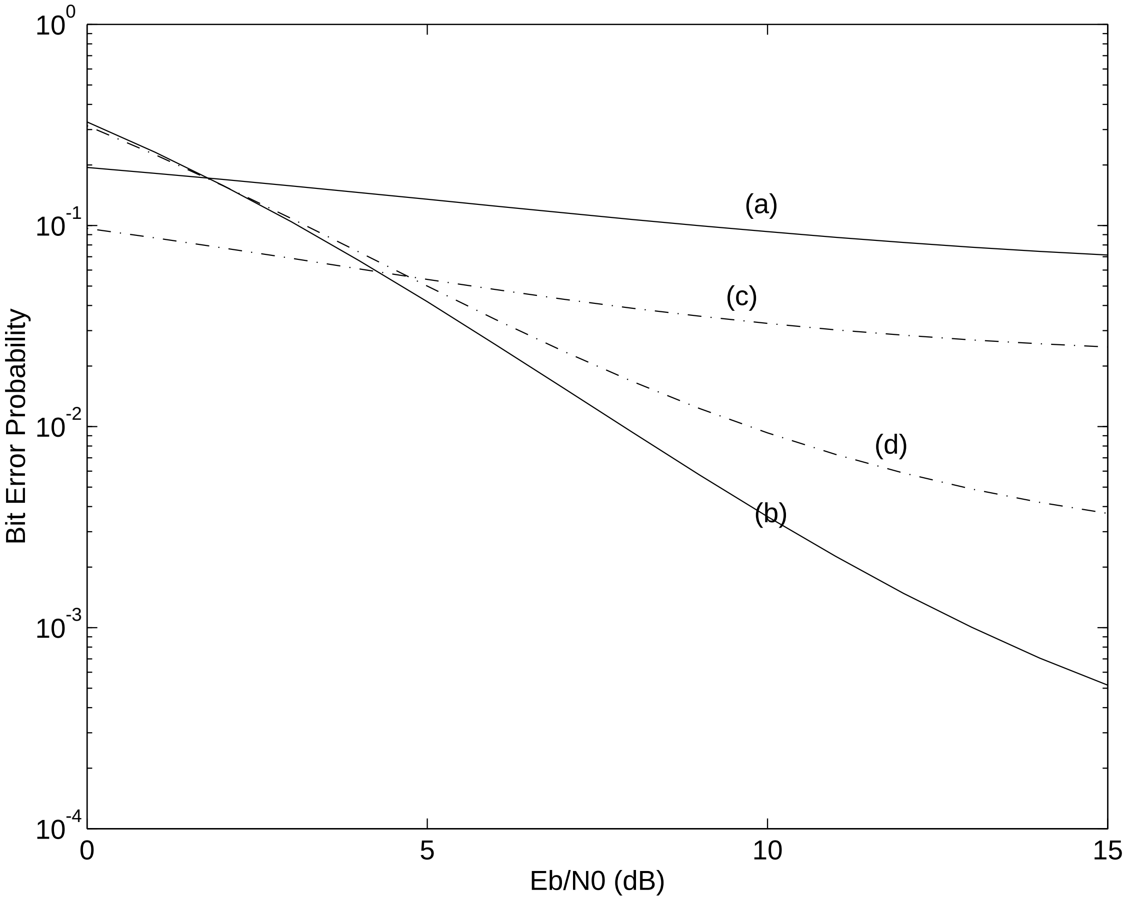

Figure 3: The effect of error control coding on MC-DS-CDMA and SC-DS-CDMA systems. $K = 70$, $M = 8$, $\tau_D = 4/W$ and $(8, 4)$ RM code is applied where coding is present. a),b) MC-DS-CDMA system without and with coding, respectively. c),d) SC-DS-CDMA system without and with coding, respectively.

interleaving is absent, the bit error probability oscillates as M increases. This is because in the multi-path fading channels, a larger M has both the desired effect of reducing MAI and the unwanted effect of strengthening the correlation in fading amplitudes. The oscillation of error probability results from the interplay of both effects as M increases, which was not observed in the analytical results due to the assumption on independent fading amplitudes. An intermediate case where the coherence bandwidth is a portion of the whole frequency band is shown in Fig. 9.

5 Conclusions

Following the above discussion, a number of conclusions can be made to serve as guidelines for system design:

- The performance of a MC-DS-CDMA system is less affected by the variation in user number than a SC-DS-CDMA system. This property makes MC-DS-CDMA

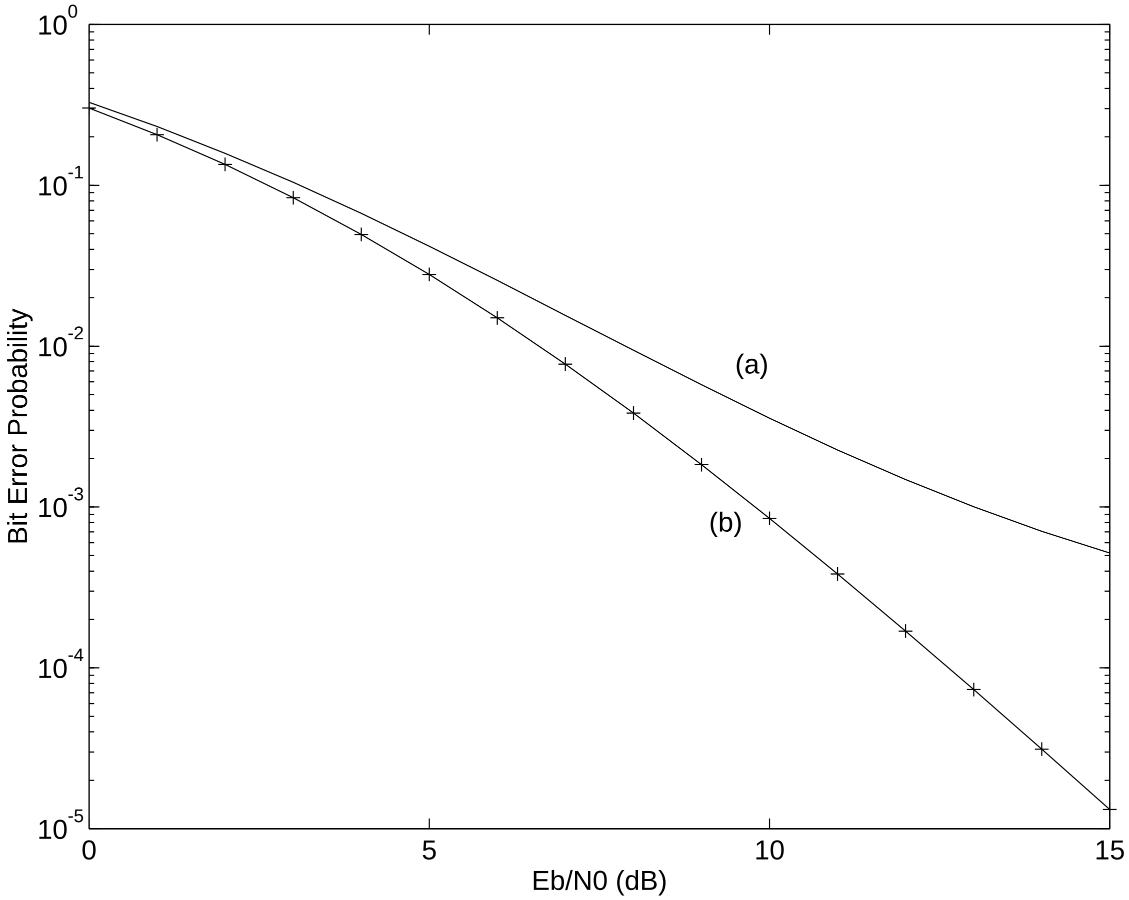

Figure 4: MC-DS-CDMA system performance using different pulse shapes. $K = 70$, $M = 8$, $\tau_D = 4/W$, and $(8,4)$ RM code is applied. a) rectangular pulse with chip time $8/W$. b) **sinc** pulse with bandwidth $W/16$.

system more suitable to operate in the environment where the service demands are relatively unstable.

- Unlike a SC-DS-CDMA system with a Rake receiver, where the performance is mainly restricted by MAI, the major performance loss of the MC-DS-CDMA system comes from multi-path fading. A properly designed error control coding scheme with soft decision decoding can effectively recover the performance loss without having to reduce the data rate.

- De-correlation of the fading amplitudes improves the performance. It is recommended that interleaving technique be used when the channel coherence bandwidth is larger than the sub-channel bandwidth.

- Unlike in AWGN channels, a larger number of sub-channels M does not always result in a better performance unless fading amplitudes are independent or interleaving technique is applied.

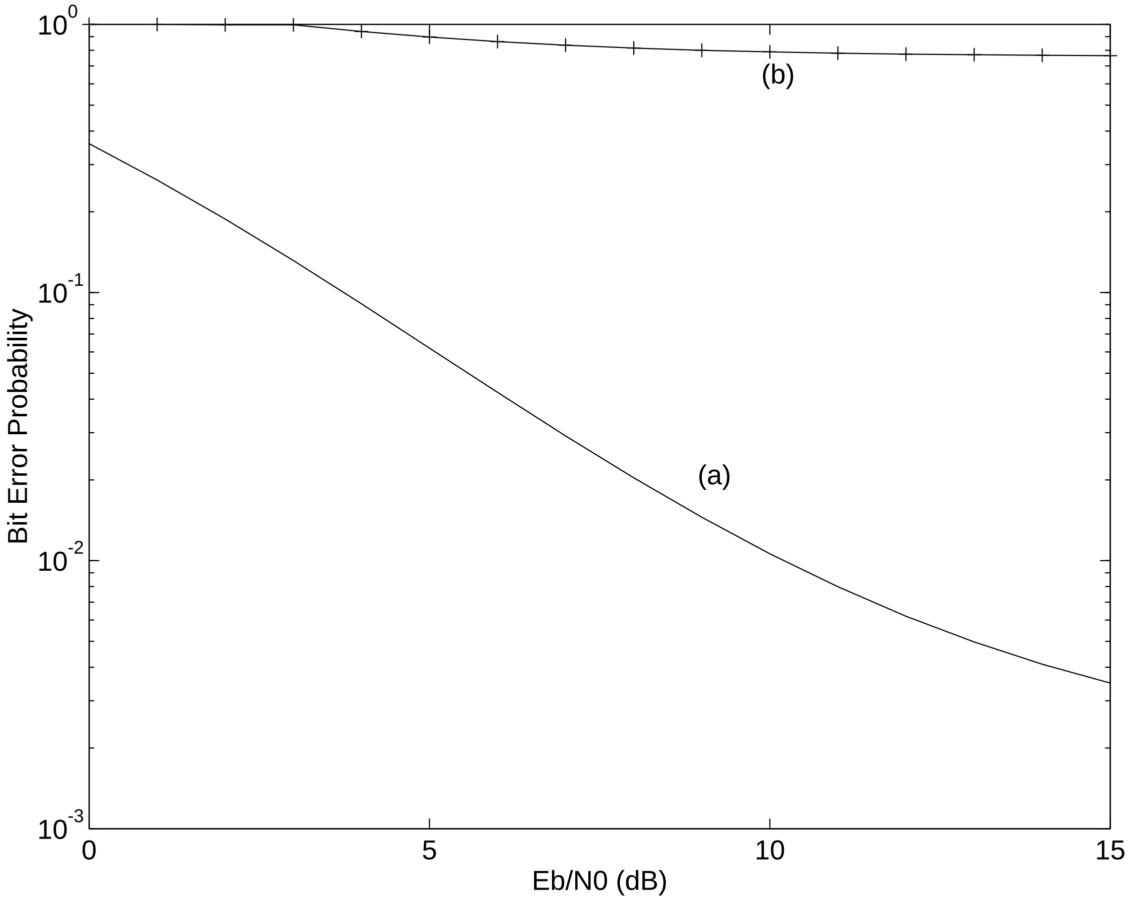

Figure 5: MC-DS-CDMA system performance under different fading amplitude correlation assumptions. $K = 70$, $M = 8$, $\tau_D = 8/W$, and $(8,4)$ RM code is applied. a) independent fading amplitudes. b) totally correlated fading amplitudes.

References

[1] L. B. Milstein, D. L. Schilling, R. L. Pickholtz, V. Erceg, M. Kullback, E. G. Kanterakis, D. S. Fishman, W. H. Biederman, and D. C. Salerno, "On the feasibility of a CDMA overlay for personal communications networks," *IEEE J. on Select. Areas in Commun.*, vol. 10, pp. 655–668, May 1992.

[2] R. L. Pickholtz, L. B. Milstein, and D. Schilling, "Spread spectrum for mobile communications," *IEEE Trans. Veh. Techn.*, vol. 40, pp. 313–321, May 1991.

[3] K. S. Gilhousen, I. M. Jacobs, R. Padovani, A. J. Viterbi, L. A. Weaver, and C. Wheatley, "On the capacity of a cellular CDMA system," *IEEE Trans. Veh. Techn.*, vol. VT-40, pp. 303–312, May 1991.

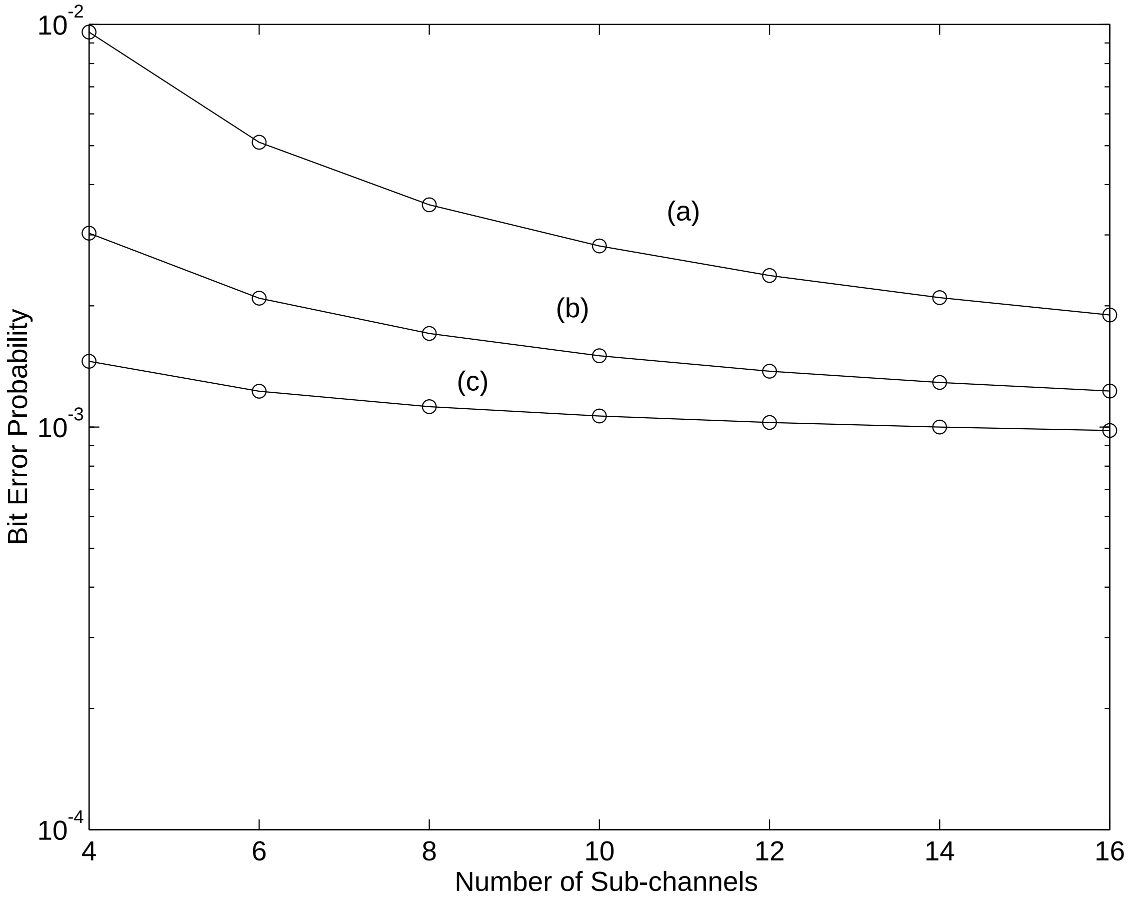

Figure 6: MC-DS-CDMA system performance versus the number of sub-channels. $K = 70$, SNR $= 10$ dB and $(8, 4)$ RM code is applied. a) $\tau_D = 4/W$, b) $\tau_D = 2/W$, c) $\tau_D = 1/W$

[4] M. B. Pursley, D. V. Sarwate, and W. Stark, "Error probability for direct sequence spread spectrum multiple-access communications-Part I: Upper and lower bounds," *IEEE Trans. Commun.*, vol. COM-30, pp. 975–984, May 1982.

[5] E. A. Geraniotis and M. B. Pursley, "Error probability for direct-sequence spread-spectrum multiple-access communications-Part II: Approximations," *IEEE Trans. Commun.*, pp. 985–995, May 1982.

[6] E. S. Sousa, "The effect of clock and carrier frequency offsets on the performance of a direct sequence spread spectrum multiple-access system," *IEEE J. on Select. Areas in Commun.*, vol. 8, pp. 580–587, May 1990.

[7] K. Fazel, "Performance of CDMA/OFDM for mobile communication system," *Proc. ICUP'93*, pp. 975–979, Oct. 93.

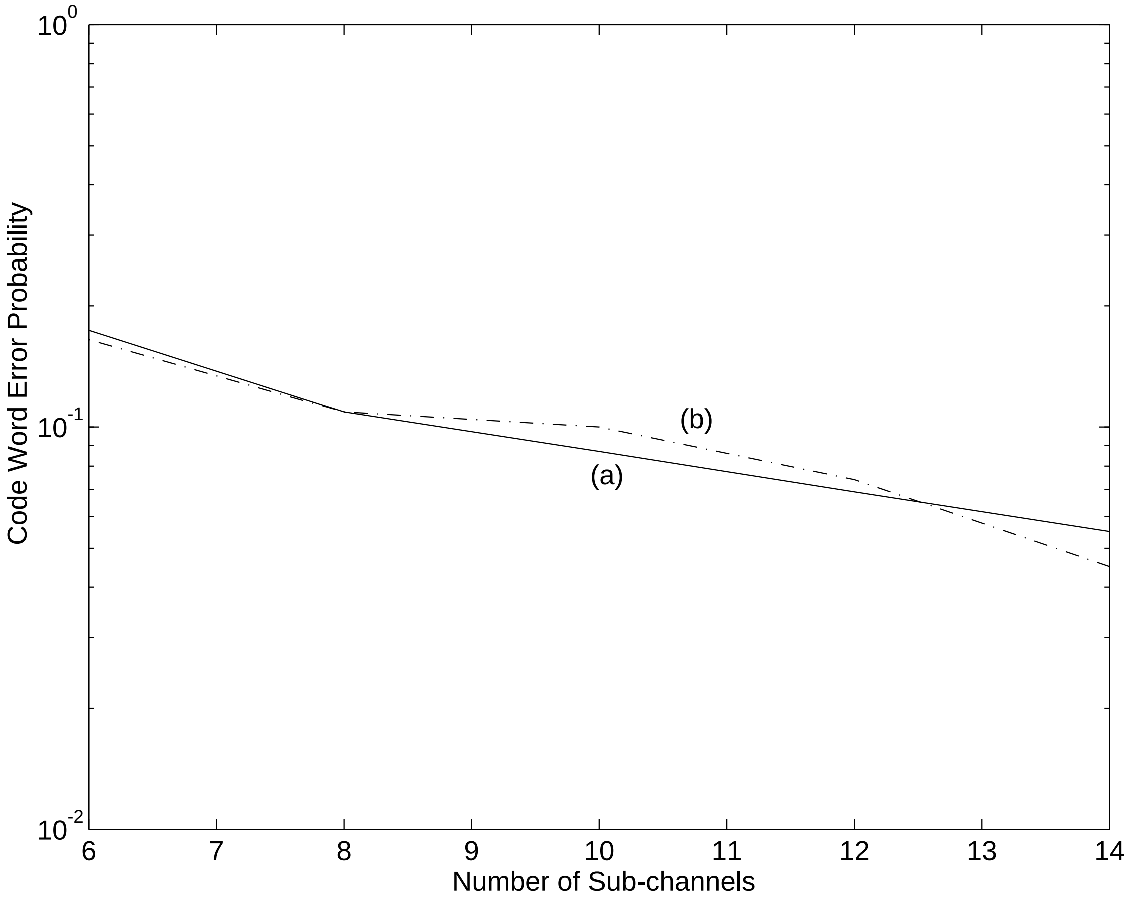

Figure 7: System performance versus the number of sub-channels.$\zeta_D = 5\mu$s, $K = 50$, SNR $= 0$ dB, and $(8, 4)$ RM code is applied. a)without interleaving, b) with interleaving.

[8] A. Chouly, A. Brajal, and S. Jourdan, "Orthogonal multicarrier techniques applied to direct sequence spread spectrum CDMA system," *Proc. GLOBECOM'93*, pp. 1723–1728, Nov. 1993.

[9] K. Fazel and L. Papke, "On the performance of convolutionally-coded CDMA/OFDM for mobile communication system," *Proc.PIMRC'93*, pp. D3.2.1–5, Dec. 1993.

[10] K. Fazel, "Performance of convolutionally coded CDMA/OFDM in a frequency-time selective fading channel and its near-far resistance," *SUPERCOMM/ICC'94*, pp. 1438–1442, May 1994.

[11] N. Yee, J. P. Linnartz, and G. Fettweis, "Multi-carrier CDMA in indoor wireless radio networks," *IEICE Trans. Commun.*, vol. E77-B, pp. 900–904, July 1994.

[12] N. Yee and J. P. Linnartz, "Wiener filtering of multi-carrier CDMA in a rayleigh fading channel," *Proc. PRIMRC'94*, pp. 1344–1347, Sept. 1994.

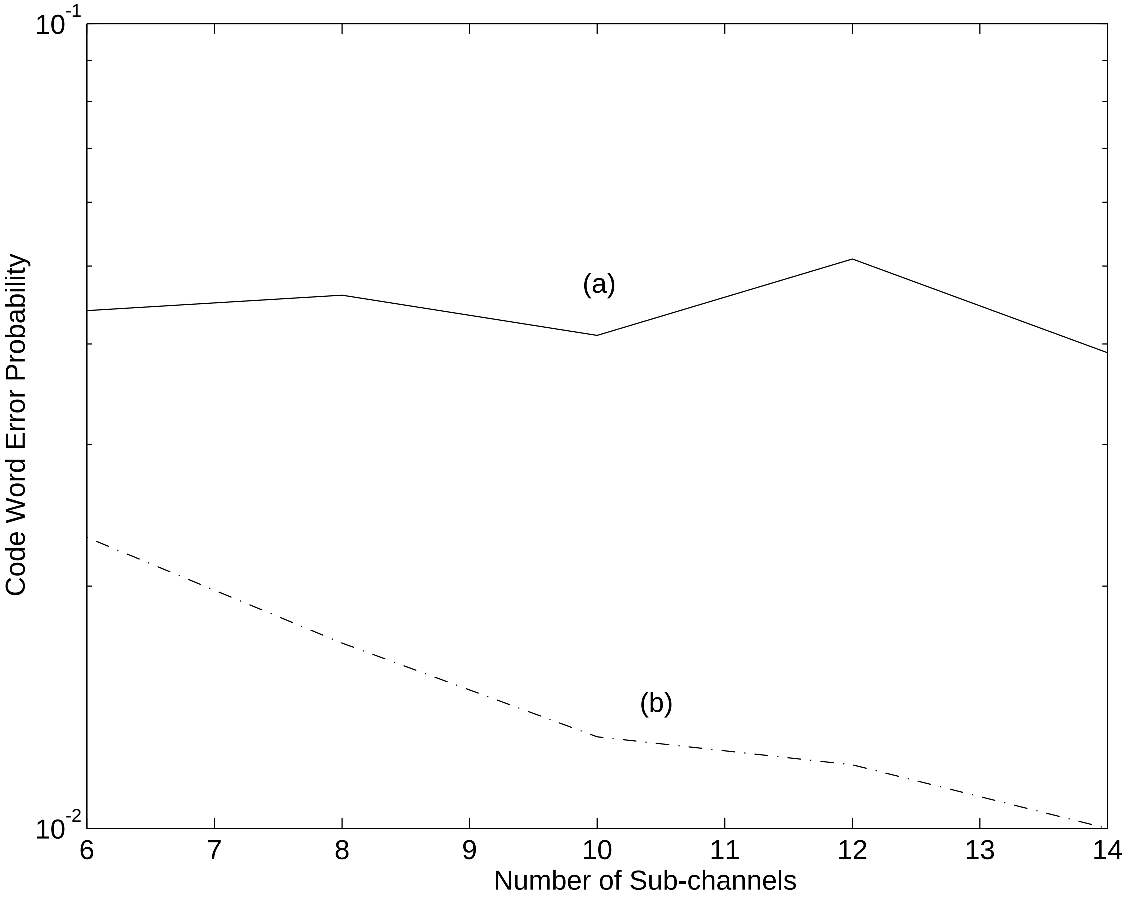

Figure 8: System performance versus the number of sub-channels. $\zeta_D = 0.8\mu$s, $K = 50$, SNR $= 0$ dB, and $(8,4)$ RM code is applied. a) without interleavingi, b) with interleaving.

[13] N. Yee and J. P. Linnartz, "Controlled equalization of multi-carrier CDMA in an indoor rician fading channel," *Proc. VTC'94*, pp. 1665–1669, Jun. 1994.

[14] Y. Bar-Ness and J. P. Linnartz, "Synchronous multi-user multi-carrier CDMA comunication system with decorrelating interference canceler," *Proc. PRIMRC'94*, pp. 184–188, Sept. 1994.

[15] V. DaSilva and E. Sousa, "Performance of orthogonal CDMA codes for quasi-synchronous communication systems," *Proc. ICUPC'93*, vol. 2, pp. 995–999, Oct. 1993.

[16] S. Kondo and L. B. Milstein, "Multicarrier DS CDMA system with cochannel interference cancellation," *Proc.VTC'94*, pp. 1640–1644, Jun 1994.

[17] S. Kondo and L. B. Milstein, "Multicarrier DS CDMA system in the presence of partial band interference," *Proc.MILCOM'94*, pp. 588–592, Oct. 1994.

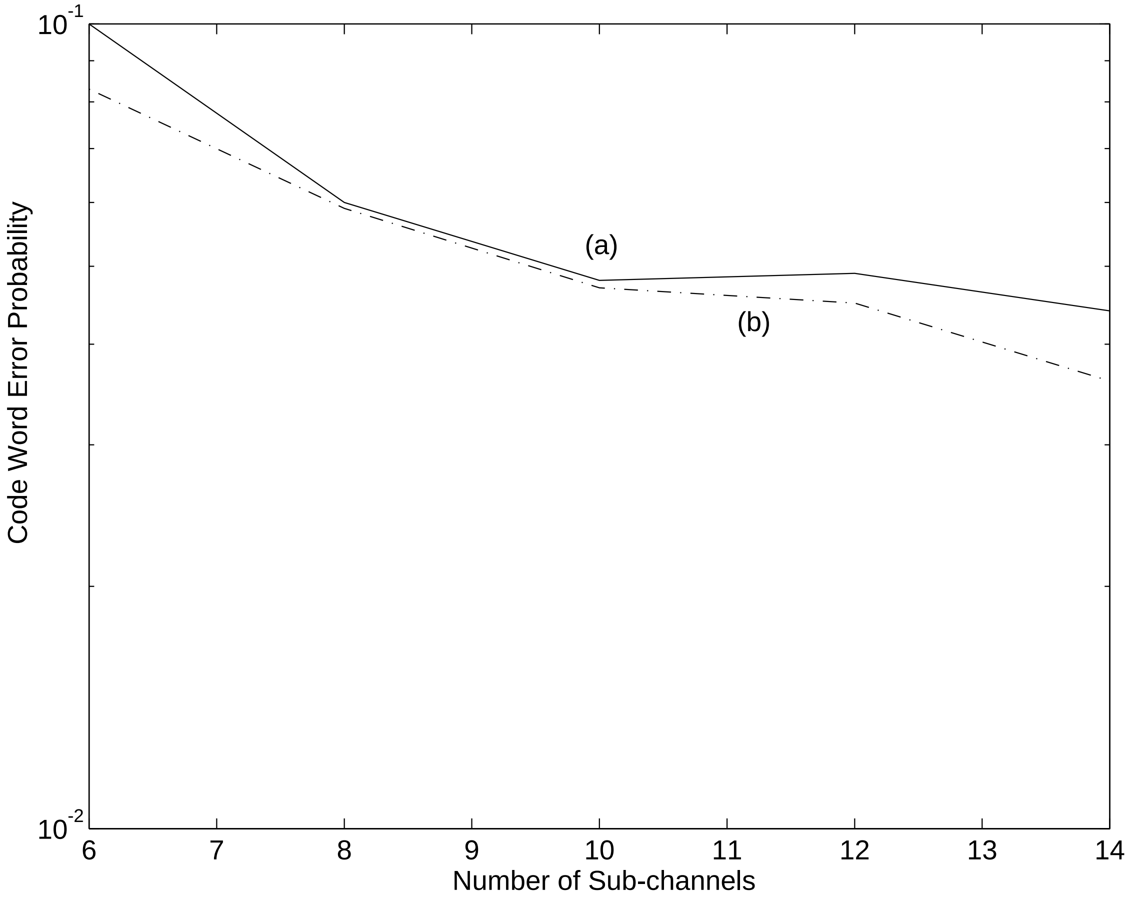

Figure 9: System performance versus the number of sub-channels. $\zeta_D = 3\mu$s, $K = 50$, SNR $= 0$ dB, and $(8, 4)$ RM code is applied. a) without interleaving, b) with interleaving.

[18] G. L. Turin, "Introduction to antimultipath techniques and their applications to urban digital radio," *Proc. IEEE*, vol. 68, pp. 328–353, Mar. 1980.

[19] E. A. Geraniotis and M. B. Pursley, "Performance of coherent direct-sequence spread-spectrum communications over specular multipath fading channels," *IEEE Trans. Commun.*, vol. COM-33, pp. 502–508, June 1985.

[20] J. G. Proakis, *Digital Communictions, 2nd Ed.* New York: Mc-Graw Hill, 1989.

[21] R. Price and P. Green, "A communication technique for multipath channels," *Proc. IRE*, pp. 555–570, Mar. 1958.

[22] D. V. Sarwate and M. B. Pursley, "Cross-correlation properties of pseudorandom and related sequences," *IEEE Proc.*, vol. 68, pp. 593–619, May 1980.

[23] R. E. Blahut, *Theory and Practice of Error Control Codes.* Addison-Wesley, 1983.